Original Article on Quantitative Imaging of Thoracic Diseases

Preliminary study on the diagnostic value of single-source dual-energy CT in diagnosing cervical lymph node metastasis of thyroid carcinoma

Yanfeng Zhao[1], Xiaolu Li[1], Lin Li[1], Xiaoyi Wang[1], Meng Lin[1], Xinming Zhao[1], Dehong Luo[1], Jianying Li[2]

[1]Department of Diagnostic Radiology, National Cancer Center/Cancer Hospital, Chinese Academy of Medical Sciences and Peking Union Medical College, Beijing 100021, China; [2]CT Research Center, GE Healthcare China, Beijing 100176, China

Contributions: (I) Conception and design: Y Zhao, L Li, D Luo; (II) Administrative support: X Zhao; (III) Provision of study materials or patients: L Li, M Lin, X Wang; (IV) Collection and assembly of data: X Wang, L Li, X Li; (V) Data analysis and interpretation: Y Zhao, L Li, J Li; (VI) Manuscript writing: All authors; (VII) Final approval of manuscript: All authors.

Correspondence to: Lin Li. Department of Diagnostic Radiology, National Cancer Center/Cancer Hospital, Chinese Academy of Medical Sciences and Peking Union Medical College, Beijing 100021, China. Email: linlin77216@sina.com.

Background: To investigate the value of single-source dual-energy spectral CT imaging in improving the accuracy of preoperative diagnosis of lymph node metastasis of thyroid carcinoma.

Methods: Thirty-four thyroid carcinoma patients were enrolled and received spectral CT scanning before thyroidectomy and cervical lymph node dissection surgery. Iodine-based material decomposition (MD) images and 101 sets of monochromatic images from 40 to 140 keV were reconstructed after CT scans. The iodine concentrations (IC) of lymph nodes were measured on the MD images and was normalized to that of common carotid artery to obtain the normalized iodine concentration (NIC). The CT number of lymph nodes as function of photon energy was measured on the 101 sets of images to generate a spectral HU curve and to calculate its slope λ_{HU}. The measurements between the metastatic and non-metastatic lymph nodes were statistically compared and receiver operating characteristic (ROC) curves were used to determine the optimal thresholds of these measurements for diagnosing lymph nodes metastasis.

Results: There were 136 lymph nodes that were pathologically confirmed. Among them, 102 (75%) were metastatic and 34 (25%) were non-metastatic. The IC, NIC and the slope λ_{HU} of the metastatic lymph nodes were 3.93±1.58 mg/mL, 0.70±0.55 and 4.63±1.91, respectively. These values were statistically higher than the respective values of 1.77±0.71 mg/mL, 0.29±0.16 and 2.19±0.91 for the non-metastatic lymph nodes (all $P<0.001$). ROC analysis determined the optimal diagnostic threshold for IC as 2.56 mg/mL, with the sensitivity, specificity and accuracy of 83.3%, 91.2% and 85.3%, respectively. The optimal threshold for NIC was 0.289, with the sensitivity, specificity and accuracy of 96.1%, 76.5% and 91.2%, respectively. The optimal threshold for the spectral curve slope λ_{HU} was 2.692, with the sensitivity, specificity and accuracy of 88.2%, 82.4% and 86.8%, respectively.

Conclusions: The measurements obtained in dual-energy spectral CT improve the sensitivity and accuracy for preoperatively diagnosing lymph node metastasis in thyroid carcinoma.

Keywords: Thyroid carcinoma; lymph node; metastasis; spectral CT

Submitted Aug 05, 2017. Accepted for publication Sep 28, 2017.
doi: 10.21037/jtd.2017.09.151
View this article at: http://dx.doi.org/10.21037/jtd.2017.09.151

Introduction

Thyroid cancer is the most common tumor in head and neck, with an increasingly high incidence. The lymph node metastasis rate of thyroid carcinoma was reported as from 36% to 90% (1-6), and its occurrence has a direct impact on staging and prognosis. At present, the method of preoperative diagnosis of lymph node metastasis mainly includes ultrasound and CT, but the two have limited specificity, even if combined there are still some limitations (7-11). The dual-energy spectral CT imaging can reconstruct material decomposition (MD) images and a set of virtual monochromatic images with photon energy ranging from 40 to 140 keV, to generate spectral HU curve, i.e., CT attenuation as function of photon energy. The added MD images and spectral HU curve is expected to help diagnose the cervical lymph node metastasis of thyroid carcinoma. The aim of this study was to investigate the value of the dual-energy spectral CT in improving the accuracy of preoperatively diagnosing lymph node metastasis of thyroid carcinoma.

Methods

Objects

This was a retrospective study. From January 2015 to December 2015, 110 patients received cervical and upper mediastinal CT scan on their first visit to our hospital due to thyroid mass. The patient admission criteria included: (I) over 18 years old; (II) postoperative pathology confirmed to have thyroid cancer; (III) no other history of cervical tumors except the thyroid tumor; (IV) no history of radiation treatment in the neck. The exclusion criteria included: (I) patients didn't receive surgical treatment or postoperative pathology confirmed to be nodular goiter, adenoma, thyroiditis and other benign lesions (22 cases); (II) pathology confirmed to be lymphoma (2 cases); (III) lymph nodes in CT images were less than 5mm and patients didn't receive cervical lymph node dissection (52 cases). Finally, 34 patients aging from 18 to 66 (42.24±14.65) years old, including 16 males (47.1%) and 18 females (52.9%), were included in the study. These patients received thyroidectomy and cervical lymph node dissection in the head and neck surgery department in our hospital. And the pathological results include 32 cases of papillary carcinoma and 2 cases of medullary carcinoma.

Imaging scanning protocol and analysis

All CT scans were performed on a Discovery CT750 HD Scanner (GE Healthcare) using the single-source, dual-energy spectral CT imaging mode with patient in the supine position and with the neck stretching as far as possible. CT scans were from the bottom of the skull to the upper margin of the aortic arch. Detailed scan protocol included: fast tube voltage switching (0.5 ms) between 80 and 140 kVp, tube current of 260 mA, pitch of 0.984 and rotation time of 0.7 s. All patients were injected with 90 mL of non-ionic contrast agent via a high-pressure syringe at a flow rate of 3 mL/s. The scan delay was 45 seconds. Both the iodine-based MD images and 101 sets of monochromatic images from 40 to 140 keV were reconstructed after CT scans at 5 mm slice thickness. These images were transferred to an advanced workstation (AW4.6. GE Healthcare) for measurement and analysis using the Gemstone Spectral Imaging (GSI) viewer image analysis software.

A radiologist (L.L.) with over 17 years' of experience in head and neck cancer diagnosis reviewed all the CT images without knowing the pathological results and made a diagnosis of lymph node metastasis with the conventional method using the following morphological criteria: (I) shortest diameter ≥5 mm on the cross-sectional plane; (II) significantly enhanced (The CT value was 30HU higher than that of muscle at the same slice); (III) containing small calcification; (IV) cystic degeneration (8,12-16).

Another doctor (Y. L.) with 5 years of experience in head and neck cancer diagnosis measured spectral-CT image related parameters by drawing region-of-interest (ROIs) on the image slice containing the primary lesions with the highest intensity and all the lymph nodes with the shortest diameter ≥5 mm, while avoiding necrosis and calcification regions (*Figures 1*,*2*). The measured Spectral CT parameters included the iodine concentration (IC) and CT attenuation value (CT number, HU) in the ROIs (17-19). IC of lymph nodes was measured on the iodine-based MD images and was normalized to that of common carotid artery to obtain the normalized iodine concentration (NIC): $NIC = IC_{lesion}/IC_{common\ carotid\ artery}$. The CT number of lymph nodes as function of photon energy was measured on the 101 sets of virtual monochromatic images to generate a spectral HU curve and to calculate its slope λ_{HU} using the following formula: λ_{HU} = CT value (40 keV) – CT value (100 keV)/(100–40), where CT value (40 keV) and CT value (100 keV) are the CT attenuation measurements at 40 and 100 keV, respectively.

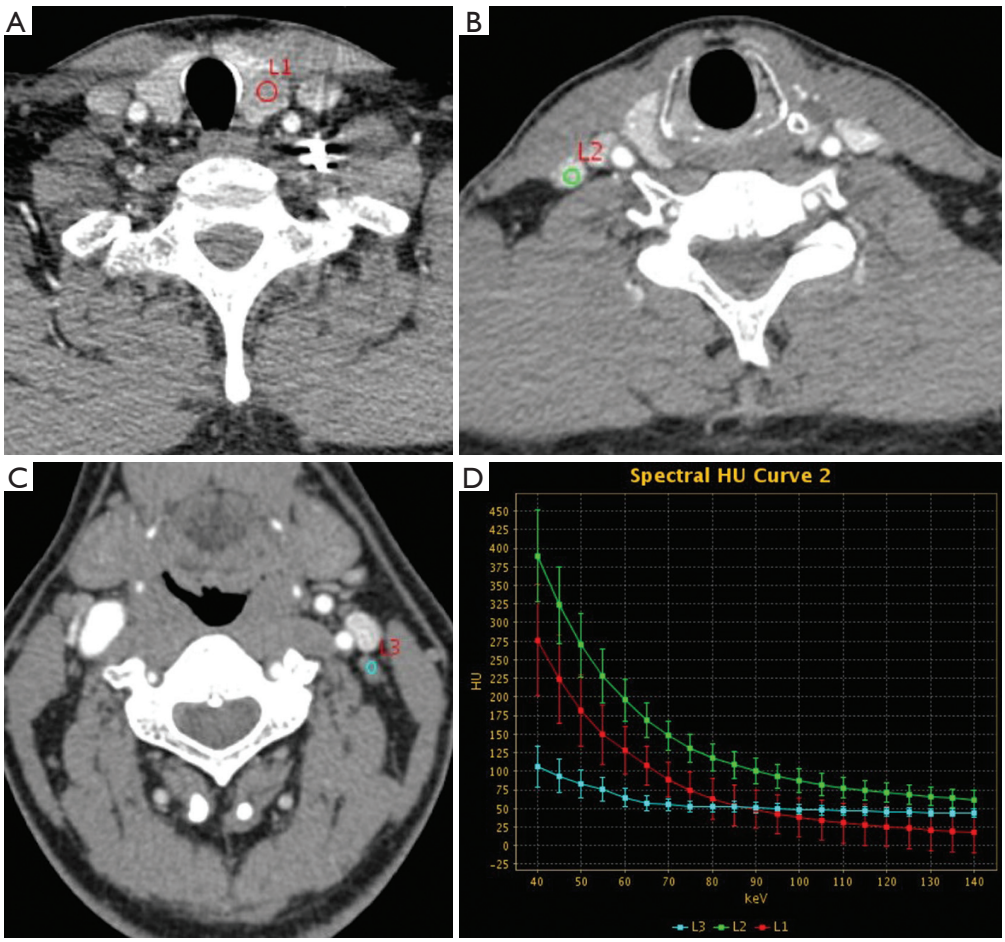

Figure 1 Male, 44 years of age with thyroid papillary carcinoma. (A) L1 is the primary tumor in the left lobe of the thyroid, with irregular shape and unclear margin. IC, NIC and λ_{Hu} were 3.24, 0.42 and 3.83 mg/mL, respectively; (B) L2 is a right cervical region IV lymph node, with regular shape and clear margin. IC, NIC, and λ_{HU} were 4.72, 0.62, and 5.55 mg/mL, respectively. The pathology was confirmed to be metastatic; (C) L3 is a left cervical region III lymph node, with regular shape and clear margin. IC, NIC, and λ_{HU} were 1.24, 0.16, and 1.42 mg/mL. The pathology was confirmed to be non-metastatic; (D) the spectral curve between 40 and 100 keV shows that the curve of metastatic lymph node is above that of the primary lesion, whereas the curve of non-metastatic lymph node is below that of the primary lesion. IC, iodine concentration; NIC, normalized iodine concentration.

Surgical pathology analysis and grouping

The radiological, surgical and pathological lymph node division all followed the Som's criteria and cervical lymph nodes were divided into 7 regions on bilateral side, with a total of 14 regions (20). The surgeons marked on the lymph nodes dissected in each region and surgical specimens were stained and diagnosed by experienced pathologists. Combining surgical and pathological results, a total of 34 patients received partial or total thyroid resection and cervical lymph node dissection, including 32 cases of papillary carcinoma and 2 cases of medullary carcinoma. All lymph nodes measured on the CT images were correlated with the pathological results according to the lymph node division during surgery, and were divided into two groups: metastasis group and non-metastasis group.

Statistical analysis

Statistical data analysis was performed using SPSS19.0 software, the count data was represented as rate, and the chi-square test (Pearson method and McNemar method) was

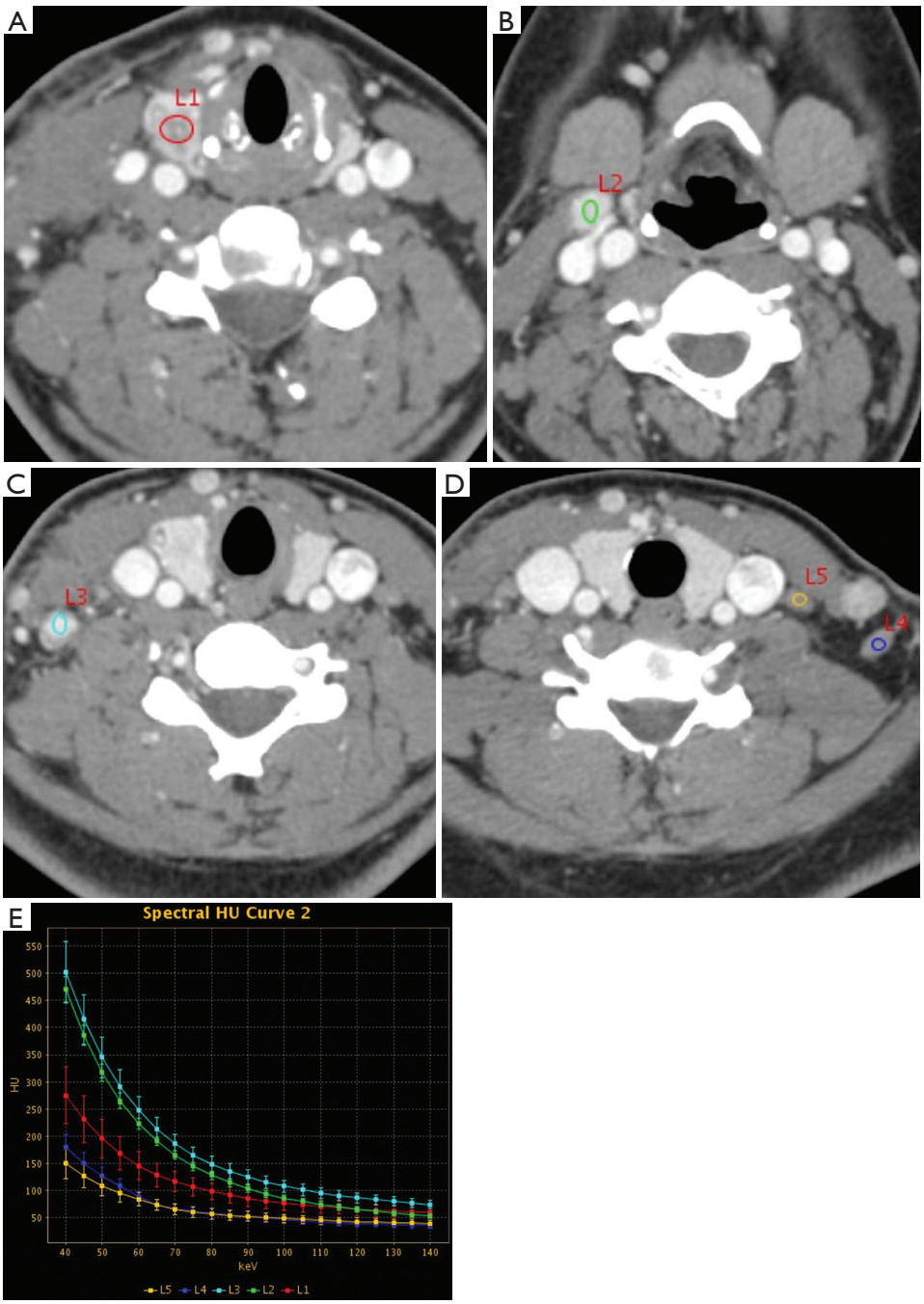

Figure 2 Female, 22 years with papillary thyroid carcinoma. (A) L1 is the primary tumor in the right lobe of the thyroid, with irregular shape and unclear margin. IC, NIC and λ_{HU} were 2.61, 0.37 and 3.09 mg/mL; (B) L2 is a right cervical region II lymph node, with regular shape and clear margin. IC, NIC, and λ_{HU} were 4.03, 0.57, and 4.97 mg/mL. The pathology was confirmed to be metastatic; (C) L3 is a right cervical region IV lymph node, with regular shape and clear margin. IC, NIC, and λ_{HU} were 4.32, 0.62, and 5.13 mg/mL. The pathology was confirmed to be metastatic; (D) L4 and L5 are left cervical region IV and V lymph nodes, both with regular shape and clear margin. IC, NIC, and λ_{HU} were 1.71, 0.24, 2.17 and 1.45, 0.20, 1.67 mg/mL, respectively. Both were confirmed to be non-metastatic; (E) the spectral curve between 40 and 100 keV shows that the spectral curve of metastatic lymph nodes (L2, L3) is above that of the primary lesion, while the spectral curve of non-metastatic lymph nodes (L4, L5) is below that of the primary tumor. IC, iodine concentration; NIC, normalized iodine concentration. IC, iodine concentration; NIC, normalized iodine concentration.

Table 1 Metastatic and non-metastatic lymph node distribution in each area

Group	II_R	II_L	III_R	III_L	IV_R	IV_L	V_R	V_L	VI_R	VI_L	VII	Total
Metastatic	8	5	14	11	19	17	4	1	13	7	3	102
Non-metastatic	6	9	5	8	1	5	0	0	0	0	0	34
Total	14	14	19	19	20	22	4	1	13	7	3	136

None of the region I lymph node was dissected among all the patients, thus not included.

Table 2 Lymph node morphological signs

Group	Shape		Margin		Calcification		Cystic degeneration	
	Regular	Irregular	Clear	Unclear	None	Presence	None	Presence
Metastatic	56 (54.9%)	46 (45.1%)	61 (59.8%)	41 (40.2%)	82 (80.4%)	20 (19.6%)	69 (67.6%)	33 (32.4%)
Non-metastatic	34 (100%)	0	34 (100%)	0	34 (100%)	0	34 (100%)	0
X^2	23.170		96.565		7.816		14.524	
P	<0.001		<0.001		0.005		<0.001	

carried out. T test was used to compare the dual-energy spectral CT parameters between the two groups, and P value less than 0.05 was considered to indicate a statistically significant difference. For the comparison among the metastatic lymph node, non-metastatic lymph node and primary lesion, the ANOVA test was used, and P value less than 0.05 was considered to indicate a statistically significant difference. The receiver operating characteristic (ROC) study was carried out for diagnosing lymph node metastasis based on either the morphological signs or Spectral CT parameters, using postoperative pathological results as the gold standard. The optimal threshold values of using Spectral CT parameters for the diagnosis were determined by ROC curves, and the sensitivity, specificity and accuracy of these thresholds were calculated, with significance level α =0.05.

Results

Size and distribution of lymph nodes

In our study, a total of 136 lymph nodes (in 34 patients) with a shortest diameter of over 5 mm were included and compared with the pathological results after neck dissection. Among them, there were 102 (75.0%) metastatic lymph nodes, and 34 (25.0%) non-metastatic lymph nodes. The shortest diameter of lymph node was 1.18±1.30 cm in the metastatic group and 0.94±1.96 cm in the non-metastatic group, without a statistically significant difference (t =–0.663, P=0.511). The distribution of lymph nodes in each region is shown in *Table 1*.

Table 1 shows that the lymph nodes in the metastatic group mainly distributed in the bilateral cervical deep chain, tracheal esophageal groove and mediastinum, ranking from more to less as region IV, III, VI, II, V and VII, and that non-metastatic lymph nodes distributed mostly in the cervical deep chain, ranking from more to less as region II, III, IV, with none in region V–VII.

Morphological signs of lymph nodes

The characteristics on shape, margin, calcification and cystic degeneration of lymph nodes in the metastatic and non-metastatic groups are shown in *Table 2*.

The sensitivity, specificity and accuracy of using irregular shape in the diagnosis of lymph node metastasis were 45.1%, 100% and 58.8%, respectively. The sensitivity, specificity and accuracy of using unclear margin were 40.2%, 100% and 55.1%, respectively. The sensitivity, specificity and accuracy of using calcification in the diagnosis of lymph node metastasis were 19.6%, 100% and 39.7%, respectively. The sensitivity, specificity and accuracy of using cystic degeneration in the diagnosis of lymph node metastasis were 32.4%, 100% and 49.3%, respectively.

Spectral parameters of lymph nodes

The dual-energy Spectral CT parameters for the lymph

node metastasis group, non-metastasis group and primary lesions are shown in *Table 3*.

There were statistically significant differences in IC, NIC and λ_{HU} between the three groups. Inter-group comparison showed significant difference of these parameters between metastatic lymph nodes and primary lesions, as well as between metastatic and non-metastatic lymph nodes (P<0.05). Between non-metastatic lymph nodes and primary lesions, there were significant differences for IC and λ_{HU} (P<0.05), while no significant difference for NIC (P>0.05).

The area under the curve (AUC) for the ROC study, the optimal cut-off value (with the maximum Youden index) and the sensitivity, specificity and accuracy of each parameter in diagnosing lymph nodes metastasis are shown in *Table 4*.

Among the three dual-energy Spectral CT parameters, the AUC of IC was the highest at 0.928. But there was no significant difference compared with the other two parameters (P>0.05). The sensitivity (83.3–96.1%) and accuracy (85.3–91.2%) of the three Spectral CT parameters were significantly higher than the sensitivity (19.6–45.1%) and accuracy (39.7–58.8%) of using the conventional CT morphological signs, with statistically significant difference (P<0.005), but the specificities of the Spectral parameters were lower than the traditional morphological signs (76.5–91.2% *vs.* 100.0%). Among the three Spectral CT parameters, the accuracy of NIC was the highest, but there was no significant difference compared with the other two parameters (P>0.05). Combining IC (>0.745), calcification and cystic degeneration, where the presence of any of the three would be diagnosed as metastatic, the sensitivity, specificity and accuracy were 93.1% (95/102), 91.2% (31/34), 92.6% (126/136). The diagnostic accuracy of combining IC and morphological signs was higher than any of the three dual-energy spectral CT parameters alone, with a significant difference compared with IC (P=0.002, McNemar method), while with no significant difference compared with NIC (P>0.05, McNemar method). Combining NIC (>0.289), calcification and cystic degeneration, where the presence of any of the three would be diagnosed as metastatic, the sensitivity, specificity and accuracy were 99.0% (101/102), 76.5% (26/34), 93.4% (127/136). The diagnostic accuracy of combining energy spectrum parameters with morphological signs was higher than any of the three dual-energy spectral CT parameters alone, with a significant difference compared with IC and slope (P=0.027, 0.022, McNemar method), while without significant difference compared with NIC (P>0.05, McNemar method).

Table 3 Dual-energy Spectral CT parameters of the lymph node metastasis group, non-metastasis group and primary lesions

Group	IC (mg/mL)	NIC	Spectral curve slope (λ_{HU})
Metastatic	3.93±1.58	0.70±0.55	4.63±1.91
Non-metastatic	1.77±0.71	0.29±0.16	2.19±0.91
Primary lesion	3.03±1.34	0.46±0.18	3.58±1.58
t[a]	10.866	6.700	9.917
P[a]	<0.001	<0.001	<0.001

[a], stands for *t*-test between metastasis group and non-metastasis group. IC, iodine concentration; NIC, normalized iodine concentration.

Discussion

Thyroid cancer is the most common tumor in the head and neck. Clinicians concern a lot about whether there is cervical lymph node metastasis, because it is closely related to surgical planning and prognosis (7,10,21,22). For patients without distant metastasis, lymph node metastasis is a key factor in determining treatment options. According to previous articles, the sensitivity, specificity and accuracy of using ultrasound, CT and ultrasound combined with CT for diagnosing lymph node metastasis are 51–82%, 88–97%, and 77–81% (2,8,13,15,16). Traditional methods of diagnosing lymph node metastasis based on morphological features mostly have high specificity but low

Table 4 Diagnostic value of four energy spectrum parameters in the diagnosis of metastatic lymph nodes

Parameters	Youden index	AUC	Cut-off value	Sensitivity (%)	Specificity (%)	Accuracy (%)
IC	0.745	0.928	>2.56	83.3	91.2	85.3
NIC	0.726	0.875	>0.289	96.1.	76.5	91.2
Spectral curve slope	0.706	0.907	>2.692	88.2	82.4	86.8

AUC, area under the curve; IC, iodine concentration; NIC, normalized iodine concentration.

sensitivity, and the overall accuracy is limited. Dual-energy Spectral CT provides not only the traditional morphological characteristics, but also material separation information and energy spectrum-related parameters. In our study, we evaluated the clinical advantages of the combination of morphological characteristics and dual-energy spectral CT parameters in improving the sensitivity and accuracy for lymph node metastasis diagnosis.

CT imaging features such as size, shape, margins (whether invasive), calcification and necrotic/cystic degeneration have been widely used to diagnose lymph node metastasis of thyroid cancer. The size of the metastatic lymph node in thyroid cancer is often small (less than 1.0 cm), bringing difficulty to diagnosing lymph node metastasis based on size (23). Although the shape and margin features of lymph nodes contribute to the diagnosis of metastasis, the signs are significantly influenced by the observer's subjective factors and have a poor stability. In our study, the sensitivity (45.1%, 40.2%) and accuracy (58.8%, 55.1%) of using the conventional CT imaging features were low, and the diagnostic value was limited. Calcification and necrotic/cystic degeneration are easy to determine on CT, have a high consistency among observers and these signs provided a high specificity (100%) in our study, but the sensitivity (19.6%, 40.2%) and accuracy (58.8%, 55.1%) were very low, which is consistent with the previous literatures (2,8,15,16), and the practical value is also limited.

At present, the application of dual-energy Spectral CT mainly includes the following four aspects: material separation, single energy imaging, energy spectral curve and the effective atomic number. In the field of medical diagnosis, the iodine map (IC) in the material separation and the slope of the curve in the energy spectral curve are often used in the diagnosis of benign and malignant lesions (17-19). In our study, all three spectral CT parameters, IC, NIC, and λ_{HU}, had a relatively high diagnostic value in the diagnosis of thyroid cancer lymph node metastasis, which was significantly higher than that of the CT morphological signs. IC was a directly measured parameter, and the other two were calculated parameters. The results of IC, NIC and λ_{HU} were consistent with previous studies in the lung, liver and pancreas (19,24-26). The IC in tumors or organs is typically a direct reflection of blood flow (27,28). However, due to the specific iodine-uptake nature of thyroid, elevated IC in thyroid may be the sum of blood-supply and the intrinsic iodine uptake by thyroid. Our results indicated that the metastatic lymph nodes had higher IC than thyroid carcinoma which in turn had higher IC than the non-metastatic lymph nodes. We hypothesize that thyroid carcinoma had abnormal blood supply that increased the IC. But this IC increase was tempered by the reduced iodine uptake ability of the thyroid carcinoma which partially offset the blood flow-induced IC increase. On the other hand, the IC increase in metastatic lymph nodes was mainly due to the increased blood supply itself. Our study showed that in the diagnosis of cervical lymph node metastasis, the AUC of IC was the highest (0.928), and the accuracy of NIC was the highest (91.2%), but the specificity of NIC (76.5%) was lower than that of IC (91.2%). On the one hand, IC is a direct measure, while NIC is the ratio of two measurements, thus IC is easier to obtain. At the same time, this study also observed that the λ_{HU} of metastatic lymph nodes (4.63±1.91) was higher than that of thyroid primary tumors (3.58±1.58), and the latter was higher than that of non-metastatic lymph nodes (2.19±0.91).

Calcification, necrosis/cystic degeneration signs on the CT are easy to recognize and highly consistent among observers. Combined with morphological signs such as calcification and necrotic/cystic degeneration, the sensitivity, specificity and accuracy of IC were increased respectively from 83.3%, 91.2%, 85.3% to 93.1%, 91.2%, 92.6%, and the sensitivity, specificity and accuracy of NIC were increased from 96.1%, 76.5%, 91.2% to 99.0%, 76.5%, 93.4%. Both IC and NIC combined with morphological signs had a diagnostic value higher than those of IC, NIC, and λ_{HU} alone in the diagnosis of lymph nodes metastasis. IC combined with morphological signs was more balanced in terms of providing high values in both sensitivity and specificity, and IC is a direct measurement, which is easy to obtain.

Limitations of this study: 136 lymph node lesions came from 34 patients, which make the data have a certain homology, reducing the reliability of the results. The number of metastatic group was significantly higher than that of non-metastatic group, which may bring bias to the results and may overestimate the sensitivity and accuracy. The combination of morphological signs and spectral CT-specific parameters did not improve the specificity of differentiating the metastatic and non-metastatic lymph nodes. This may also because the sample size was small and the distribution between the metastatic and non-metastatic lymph nodes was significantly uneven. Also, we didn't compare the accuracy of dual-energy Spectral CT parameters with the accuracy of ultrasound diagnosis.

In conclusion, compared with CT morphological signs, the dual-energy Spectral CT parameters have a high value for the diagnosis of thyroid cancer cervical lymph node

metastasis, and are less affected by the observers' subjective judgment. Among them, IC is the most readily available spectral parameters. Combining CT morphological signs such as calcification and necrotic/cystic degeneration with Spectral CT specific parameters such as IC further improves the diagnostic accuracy.

Acknowledgements

Funding: This work was supported by Beijing Hope Run Special Fund of China Cancer Research Foundation (CCRF) (No. LC2016A13).

Footnote

Conflicts of Interest: The authors have no conflicts of interest to declare.

References

1. Sherman SI. Thyroid carcinoma. Lancet 2003;361:501-11.
2. Kim E, Park JS, Son KR, et al. Preoperative diagnosis of cervical metastatic lymph nodes in papillary thyroid carcinoma: comparison of ultrasound, computed tomography, and combined ultrasound with computed tomography. Thyroid 2008;18:411-8.
3. González HE, Cruz F, O'Brien A, et al. Impact of preoperative ultrasonographic staging of the neck in papillary thyroid carcinoma. Arch Otolaryngol Head Neck Surg 2007;133:1258-62.
4. Brown RE, Harave S. Diagnostic imaging of benign and malignant neck masses in children-a pictorial review. Quant Imaging Med Surg 2016;6:591-604.
5. Yuan J, Lo G, King AD. Functional magnetic resonance imaging techniques and their development for radiation therapy planning and monitoring in the head and neck cancers. Quant Imaging Med Surg 2016;6:430-48.
6. Li L, Wáng YX, Shi L, et al. Primary thyroid lymphoma: CT findings of a rare malignant tumor with pathologic correlations. Transl Cancer Res 2017;6:578-87.
7. Conzo G, Docimo G, Mauriello C, et al. The current status of lymph node dissection in the treatment of papillary thyroid cancer. A literature review. Clin Ter 2013;164:e343-6.
8. Lee DW, Ji YB, Sung ES, et al. Roles of ultrasonography and computed tomography in the surgical management of cervical lymph node metastases in papillary thyroid carcinoma. Eur J Surg Oncol 2013;39:191-6.
9. Yoo YH, Kim JA, Son EJ, et al. Sonographic findings predictive of central lymph node metastasis in patients with papillary thyroid carcinoma: influence of associated chronic lymphocytic thyroiditis on the diagnostic performance of sonography. J Ultrasound Med 2013;32:2145-51.
10. Jin LX, Moley JF. Surgery for lymph node metastases of medullary thyroid carcinoma: A review. Cancer 2016;122:358-66.
11. Tam AA, Kaya C, Ucler R, et al. Correlation of normal thyroid ultrasonography with thyroid tests. Quant Imaging Med Surg 2015;5:569-74.
12. Mack MG, Rieger J, Baghi M, et al. Cervical lymph nodes. Eur J Radiol 2008;66:493-500.
13. Kim DW, Choo HJ, Lee YJ, et al. Sonographic features of cervical lymph nodes after thyroidectomy for papillary thyroid carcinoma. J Ultrasound Med 2013;32:1173-80.
14. Yoon JH, Kim JY, Moon HJ, et al. Contribution of computed tomography to ultrasound in predicting lateral lymph node metastasis in patients with papillary thyroid carcinoma. Ann Surg Oncol 2011;18:1734-41.
15. Choi YJ, Yun JS, Kook SH, et al. Clinical and imaging assessment of cervical lymph node metastasis in papillary thyroid carcinomas. World J Surg 2010;34:1494-9.
16. Wu CW, Dionigi G, Lee KW, et al. Calcifications in thyroid nodules identified on preoperative computed tomography: patterns and clinical significance. Surgery 2012;151:464-70.
17. De Cecco CN, Darnell A, Rengo M, et al. Dual-energy CT: oncologic applications. AJR Am J Roentgenol 2012;199:S98-S105.
18. Liu X, Ouyang D, Li H, et al. Papillary thyroid cancer: dual-energy spectral CT quantitative parameters for preoperative diagnosis of metastasis to the cervical lymph nodes. Radiology 2015;275:167-76.
19. Lv P, Lin XZ, Li J, et al. Differentiation of small hepatic hemangioma from small hepatocellular carcinoma: recently introduced spectral CT method. Radiology 2011;259:720-9.
20. Som PM, Curtin HD, Mancuso AA. An imaging-based classification for the cervical nodes designed as an adjunct to recent clinically based nodal classifications. Arch Otolaryngol Head Neck Surg 1999;125:388-96.
21. Lesnik D, Cunnane ME, Zurakowski D, et al. Papillary thyroid carcinoma nodal surgery directed by a preoperative radiographic map utilizing CT scan and ultrasound in all primary and reoperative patients. Head Neck 2014;36:191-202.
22. Mamelle E, Borget I, Leboulleux S, et al. Impact of prophylactic central neck dissection on oncologic outcomes of papillary thyroid carcinoma: a review. Eur

Arch Otorhinolaryngol 2015;272:1577-86.
23. Randolph GW, Duh QY, Heller KS, et al. The prognostic significance of nodal metastases from papillary thyroid carcinoma can be stratified based on the size and number of metastatic lymph nodes, as well as the presence of extranodal extension. Thyroid 2012;22:1144-52.
24. Yu Y, He N, Sun K, et al. Differentiating hepatocellular carcinoma from angiomyolipoma of the liver with CT spectral imaging: a preliminary study. Clin Radiol 2013;68:e491-7.
25. Lin XZ, Wu ZY, Li WX, et al. Differential diagnosis of pancreatic serous oligocystic adenoma and mucinous cystic neoplasm with spectral CT imaging: initial results. Clin Radiol 2014;69:1004-10.
26. Hou WS, Wu HW, Yin Y, et al. Differentiation of lung cancers from inflammatory masses with dual-energy spectral CT imaging. Acad Radiol 2015;22:337-44.
27. Miles KA. Tumour angiogenesis and its relation to contrast enhancement on computed tomography: a review. Eur J Radiol 1999;30:198-205.
28. Turner HE, Harris AL, Melmed S, et al. Angiogenesis in endocrine tumors. Endocr Rev 2003;24:600-32.

Cite this article as: Zhao Y, Li X, Li L, Wang X, Lin M, Zhao X, Luo D, Li J. Preliminary study on the diagnostic value of single-source dual-energy CT in diagnosing cervical lymph node metastasis of thyroid carcinoma. J Thorac Dis 2017;9(11):4758-4766. doi: 10.21037/jtd.2017.09.151